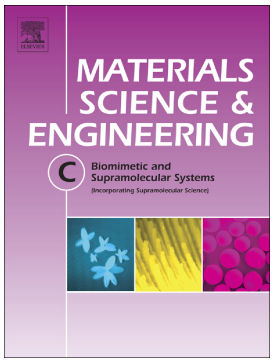

A spectroscopic and thermal investigation into the relationship between composition, secondary structure and physical characteristics of electrospun zein nanofibers

Y.H. Wang, M. Zhao, S.A. Barker, P.S. Belton, D.Q.M. Craig

PII: S0928-4931(17)34111-5
DOI: https://doi.org/10.1016/j.msec.2018.12.134
Reference: MSC 9244

To appear in: *Materials Science & Engineering C*

Received date: 14 October 2017
Revised date: 29 June 2018
Accepted date: 28 December 2018

Please cite this article as: Y.H. Wang, M. Zhao, S.A. Barker, P.S. Belton, D.Q.M. Craig , A spectroscopic and thermal investigation into the relationship between composition, secondary structure and physical characteristics of electrospun zein nanofibers. Msc (2019), https://doi.org/10.1016/j.msec.2018.12.134

A Spectroscopic and Thermal Investigation into the Relationship between Composition, Secondary Structure and Physical Characteristics of Electrospun Zein Nanofibers

Wang, Y.H.[1], Zhao, M.[2], Barker, S.A.[2], Belton, P.S.[3], Craig, D.Q.M.[2]*

1. School of Pharmacy, Heilongjiang University of Chinese Medicine, 24 Heping Road, Harbin 150040, China

2. University College London School of Pharmacy, 29-39 Brunswick Square, London WC1N 1AX, UK

3. School of Chemistry, University of East Anglia, Norwich, Norfolk NR4 7TJ, UK

Correspondence author: Duncan Q.M. Craig: duncan.craig@ucl.ac.uk

KEYWORDS: Electrospinning, nanofiber, zein, plasticizer, casein, secondary structure.

ABSTRACT

Electrospun zein nanofibers have attracted interest as drug delivery systems due to their propensity for controlled drug release, flexible structure and low toxicity. However, comparatively little is known regarding the relationship between production method and fiber characteristics, both in terms of fiber architecture and protein structure. Here we use a range of imaging and spectroscopic techniques to elucidate the effects of solvent composition on zein secondary structure, fiber diameter and fiber integrity, plus we utilize the new technique of transition temperature microscopy to examine the thermal properties of the fibers. Zein nanofibers were prepared using ethanol, acetic acid and water mixes as solvents, alone and with plasticizers (polyethyelene glycol, glycerol) and casein. Electrospinning was performed under controlled conditions and the products characterized using scanning electron microscopy (SEM), attenuated total reflection Fourier Transform infrared spectrometry (ATR - FTIR) and transition temperature microscopy (TTM). The choice of solvent, concentration and voltage, alongside the presence of additives (plasticizers and casein) were noted to influence both the diameter of the fibers and the tendency for bead formation. A relationship was noted between protein secondary structure and fiber architecture, with an enhanced β-sheet content, enhanced by the inclusion of casein, being associated with higher beading. In addition, thermal imaging of electrospun zein fiber mats was successfully achieved using TTM via two dimensional mapping of the softening temperatures across the spun samples, in particular demonstrating the plasticizing effects of the polyethylene glycol and glycerol.

INTRODUCTION

Zeins are seed storage proteins, accounting for more than 50% of the protein content of maize endosperms. While they have limited human nutritional value due to the deficiency of essential amino acids (lysine and tryptophan in particular), they are a major source of nitrogen to the embryos during seed germination. The zeins have found wide application in the textile, food and, more recently, pharmaceutical arenas as a versatile industrial polymer due to their low toxicity, favorable water permeation properties, sustainable production and biodegradable nature[1-3].

While frequently referred to in the singular, zeins are composed of a range of materials and may be classified into fractions (α, β, γ and δ) according to their solubility and sequence homology, with the α fraction representing more than 70% of the total zein composition; this fraction is alcohol soluble and is considered to be a member of the prolamin genetic family[4]. The α zeins are largely composed of two homologous fractions with approximate molecular weights of 19 and 22 kDa respectively. In terms of secondary structure, the zeins show a high α helix content, resulting in elongated structures of approximately 14nm in length. However, the zeins may also exist in an antiparallel β sheet conformation, with interchange between the two conformations possible on processing. Forato et al[5] calculated the proportion of α coils and β sheets in α zein and compared those proportions in alcoholic solution and the solid state, finding broad similarities between the two. More specifically, FTIR studies on solid systems indicated an α helix content of 43% and β sheet content of 28% for the sample in question, although circular dichroism studies yielded lower values for the β content in solution.

Zeins have attracted interest as materials for electrospinning, a process used for the production of nanofibers. More specifically, a high voltage source is used to inject charge across the meniscus tip of a polymer solution extruded from a syringe. As the electrostatic attraction between the oppositely charged liquid and collector and the electrostatic repulsions between like charges in the liquid become stronger, the leading edge of the solution changes from a rounded meniscus to a cone (the Taylor cone). A fiber jet is eventually ejected from the Taylor cone as the electric field strength exceeds the surface tension of the liquid. The fiber jet travels through the atmosphere allowing the solvent to evaporate, thus leading to the deposition of solid polymer fibers on the

collector[6]. Fibers produced using this process typically have several advantages such as an extremely high surface-to-volume ratio, tunable porosity, and malleability to conform to a wide variety of sizes and shapes; in addition the composition may be relatively easily controlled to achieve the desired functionality. Electrospun fibers have been successfully applied in tissue engineering and drug delivery[7] and such systems continue to attract interest as the applications of nanofabricated materials develop.

Several groups have successfully produced electrospun zein fibers for tissue engineering and drug delivery applications[8-17]. The published studies are mostly related to the effects of production parameters on zein electrospinning[8-10], crosslinking of zein nanofibers[11-12] and incorporation of supplementary polymers and macromolecules[13-17]. More recently, studies within the pharmaceutical and biomedical arena have investigated the use of zein fibers as a means of delivering antibiotics such as tetracycline to biofilms[18] and the delivery of vaccarin to wounds[19].

An aspect of zein nanofiber production that has not been widely studied has been the interplay between the composition, the secondary structure and the characteristics of the manufactured fibers. The secondary structure, and in particular the α helix to β sheet ratio, could conceivably have a profound influence on spinnability due to the differences in entanglement one would anticipate from these differing conformations. Indeed, it has been reported that an increase in the β-sheet content of the zein can render the protein more flexible and easily elongated[20]. For the fiber characteristics, issues such as beading and fiber diameter are obvious considerations; however, we would argue that the thermal properties are also extremely important as these will determine flexibility and release, particularly via consideration of the glass transitional properties.

The objective of this study was therefore to systematically investigate the effects of different solvents, zein concentrations and additives (plasticizers and casein) on the structural (in terms of both molecular conformation and fiber characteristics) and thermal properties of electrospun zein nanofibers, with a particular view to examining how these considerations may interplay together. Previously, aqueous ethanol, N,N-dimethylformamide (DMF), trifluoroethanol (TFE) and aqueous acetic acid (AA) have been used as solvents[8,9,13,14,15]. However, given the potential biomedical uses of these systems, aqueous ethanol and aqueous acetic acid were chosen for this work for toxicity

reasons. Similarly, polyethylene glycol (PEG) and glycerol (GLY) are plasticizers most commonly used to improve mechanical properties and other characteristics of zein films[21-24] and both have favourable toxicological profiles, hence were utilized here. Casein, the major protein in milk, has been reported to have the ability to increase and stabilize the β-sheet structure of zein[25], leading to more favorable viscoelastic properties, hence was also studied here as an additive.

The nanofibers produced in this work were characterized by scanning electron microscopy and image analysis to evaluate fiber integrity and size, and by spectroscopic methods to assess the α-helix and β-sheet contents. We used Attenuated Total Reflection Fourier Transform Infrared Spectrometry (ATR-FTIR) for this quantification due to the earlier validation studies[4,5] which showed this to be an effective method for measuring these parameters in the solid state; given the focus on the fiber product this was a necessary prerequisite to the choice of approach.

The approach of transition temperature microscopy (TTM) was used to assess the thermal transitions of the fiber mat; this will represent the first use of the technique in the nanofiber field. In brief, the method involves the application of a temperature controlled AFM tip[26] across a sample in a two dimensional pattern across the surface. The movement of the tip as a function of temperature is monitored via a piezoelectric sensor, thereby allowing the softening points to be measured at a series of locations. By mapping these softening point across the mesh surface both the nature and properties of the material can potentially be identified and characterized at a submicron scale of scrutiny. Overall, therefore, our aim is not just to identify suitable parameters for zein fiber production but also to explore correlations between production parameters and structural characteristics of the fibers, both in terms of architecture and fundamental molecular properties.

EXPERIMENTAL SECTION

Materials and solution preparation. Commercial zein (Z3625), casein, PEG 400, anhydrous glycerol (GLY) and acetic acid (AA) were purchased from Sigma-Aldrich Company Ltd (Gillingham, UK). The formulations used were prepared as shown in Table 1; all solutions were prepared by magnetic stirring for one hour.

Table 1. *Composition of zein formulations used for electrospinning*

Formulation name	Component						
	Zein (g)	Casein (g)	PEG (g)	GLY (g)	Ethanol (mL)	AA (mL)	Water (mL)
30:70 ZE	30				70		30
30:35:35 ZEA	30				35	35	30
30:70 ZA	30					70	30
40:70 ZA	40					70	30
50:70 ZA	50					70	30
60:70 ZA	60					70	30
40:6:70 ZPA	40		6			70	30
40:6:70 ZGA	40			6		70	30
39:1:70 ZCA	39	1				70	30
37:3:70 ZCA	37	3				70	30
35:5:70 ZCA	35	5				70	30

Determination of Solution Properties. The viscosities of the polymer solutions were investigated using a rheometer (AR1000-N,TA Instruments, USA) at a controlled shear rate between 2 and 400 s^{-1}. The temperature was controlled at 27 ℃. The electrical conductivity of the polymer solutions was measured using a digital conductivity meter (DIST 4, HANNA,USA).

Electrospinning. A NanoFiber Production System (NEU-202-B2E, NanoLabInstruments (M) SdnBhd, Malaysia) was used to produce fibers. Sytems investigating the different solvents and

zein concentrations were processed at a constant applied voltage of 25 kV, a feed rate of 0.5 mL/h, a distance between the needle tip and the collector of 15 cm and an ambient temperature of 27℃. The systems containing plasticizers and casein were processed at a constant applied voltage of 20 kV, feed rate of 0.5 mL/h, distance between needle tip and collector of 15 cm and ambient temperature of 27℃. Aluminium foil was used as the collection material. Samples were dried at 30ºC for a further hour following preparation.

Characterization of Electrospun Fibers.

Scanning Electronic Microscopy (SEM). The morphology of the electrospun fiber was evaluated using a scanning electron microscope (SEM) (FEI Quanta 200F, Eindhoven, The Netherlands). Square pieces of the electrospun fibers were attached to aluminium stubs and sputter coated with gold (Quorum Q150T Sputter Coater) under a nitrogen atmosphere. The average fiber diameter for each sample of the electrospun fibers was determined by Image J software (National Institutes of Health, USA), measuring at least 100 fibers per sample.

Attenuated Total Reflection Fourier Transform Infrared Spectrometry (ATR-FTIR). A Vertex 70 spectrometer (Bruker Optics, Coventry, U.K.) with a Golden Gate MkII ATR Accessory from Specac Ltd. (Orpington, U.K.) was used to scan the electrospun fibers over the wavenumber range of 600-4000cm^{-1}. Samples were placed on the ATR accessory and carefully pressed down to ensure good contact with the ATR crystal. Each measurement was an average of 16 scans at 4 cm^{-1} resolution. Three replicates of each sample were taken using the empty ATR crystal as a reference, and the secondary structures were estimated by second-derivative and Gaussian curve fitting of the amide I band in the regions of 1600−1700 cm^{-1} using OriginPro 9.0 software (OriginLab, USA). The percentage of secondary structure was calculated on the basis of the area under the curve of deconvoluted Gaussian bands. All the deconvolutions were carried out with an R^2 of 0.999.

Transition Temperature Microscopy (TTM). TTM measurements were performed over a selected area on a sample surface using a Veeco diCaliber scanning probe microscope head (Veeco, CA, USA) equipped with a thermal nanoprobes (AN-2 probes, Anasys Instruments, Santa Barbara, CA, USA). The probe was calibrated for temperature by supplying a scanning voltage profile while in contact with polymeric materials with known melting points. The sample surface was imaged with an optical microscope. Each measurement stopped when a thermal event was detected. These

measurements were carried out on a dedicated system (Vesta, Anasys Instruments, Santa Barbara, CA, USA). Transition temperature maps were measured over a 10 μm × 10 μm area, and each nanoTA measurement was carried out from room temperature until the transition temperature was detected. After each measurement, the probe was retracted and moved to the next location. All nanoTA measurements were carried out at a heating rate of 10°C s^{-1}. At least four frames were selected for each sample, with broad agreement between images being obtained.

RESULTS AND DISCUSSION

Solution properties and morphology of the electrospun zein nanofibers

As solution conductivity, viscosity and surface tension significantly influence fiber formation and affect fiber size and morphology of electrospun fibers[6], these parameters were measured and are presented in Figure 1, showing data for the different solvents, zein concentrations, plasticizers and casein contents. In general, the solutions were found to be mildly dilatant in nature, with the measured viscosity increasing with shear rate. The exception to this was the 30:70 ZE system, whereby a marked increase in viscosity was observed as the shear rate increased.

In terms of the choice of solvent, the highest viscosity values were found with ethanol as opposed to acetic acid systems; at a shear rate of 300 s^{-1}, the apparent viscosities were 0.29±0.07 Pa.s, 0.14±0.01 Pa.s and 0.11±0.01Pa.s for 30:70 ZE, 30:35:35 ZEA and 30:70 ZA respectively. Interestingly, the conductivity showed a maximum for the 30:35:35 ZEA mixed systems (1.59±0.01mS), with the 30:70 ZE and 30:70 ZA systems showing very similar values (1.43±0.01mS and 1.44±0.02mS respectively). On increasing the zein concentration, the viscosity increased and conductivity decreased, while PEG caused an increase in viscosity and both PEG and GLY decreased the conductivity. Similarly, although the system with a low level of casein (39:1:70 ZCA) showed no change compared to the zein-alone formulation (40:70 ZA), higher levels of casein caused an increase in viscosity and a decrease in conductivity.

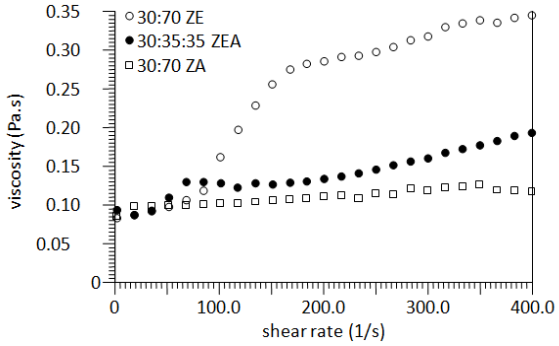

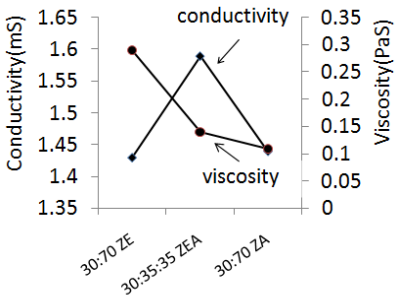

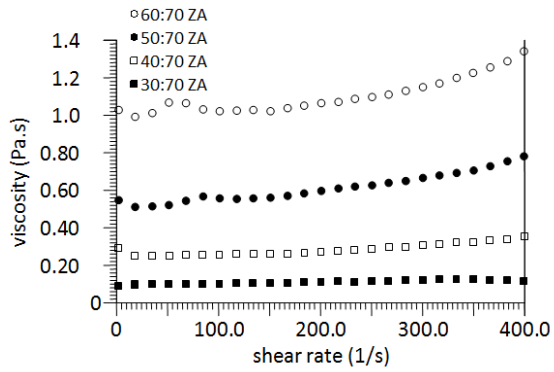

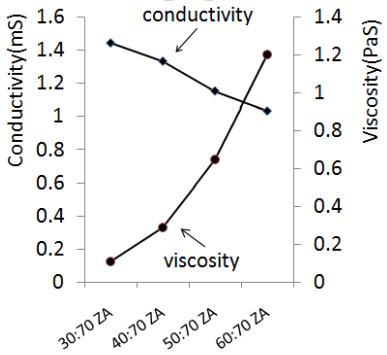

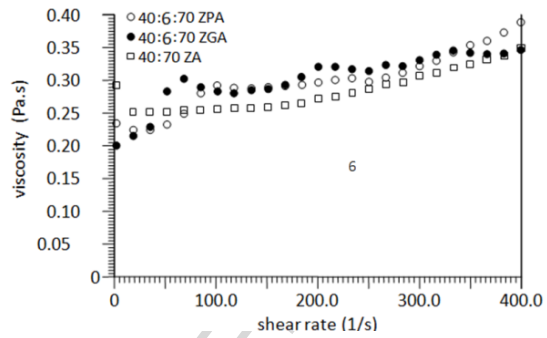

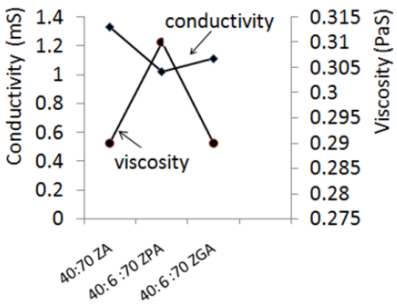

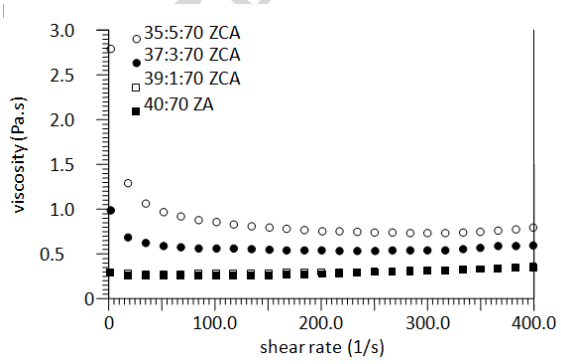

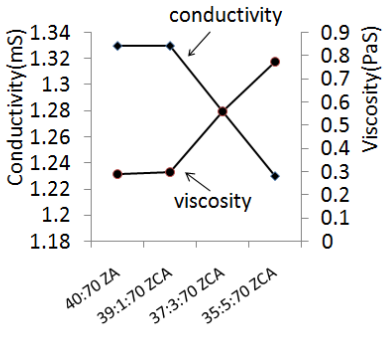

Figure 1.*The dependence of viscosity on shear rate (in the left hand column), and the conductivity and apparent viscosity at a shear rate of 300s^{-1} (in the right hand column) for electrospun zein solutions. From top to bottom: varying solvents, zein concentrations, plasticizer addition, casein addition.*

The relationship between conductivity, viscosity and nanofiber formation is complex, but in general if the viscosity is too low then continuous fiber formation is impeded, while if it is too high needle clogging occurs[6]. Similarly, there has been a reported inverse relationship between conductivity and fiber diameter[6,11]. In the present case, clogging was indeed observed for the ethanolic systems, hence acetic acid was used as the base solvent for subsequent studies.

Examination of Figure 2 indicates the morphology of the fibers produced, while Figure 3 presents the fiber diameter values. The ethanol-based systems were clearly of higher diameter, although beads were observed for some of the acetic acid systems. Beading is a well-known phenomenon in the electrospinning field and is closely related to solution concentration and viscosity. It has been found that a mixture of beads and fibers is obtained at low solution concentration and as the solution concentration increases, the shape of the beads changes from spherical to spindle-like and finally uniform fibers, with increased diameters being formed as a result of the higher viscosity[27-29]. Selling et al[30] reported that zein fibers produced from acetone/water solvent systems were much more prone to beading than equivalent ethanol systems, attributing this to the higher dielectric constant of the former.

When the zein concentration was increased (30:70 ZA to 60:70 ZA), the conductivity decreased from 1.44±0.02 mS to 1.03±0.02 mS, but the apparent viscosity at 300 s^{-1} increased from 0.11±0.01 to 1.20±0.10 Pa.s (Figure 1). Significantly, however, bead-free fibers were produced at concentrations at or above 40:70 ZA (Figure 2), while the diameter of these fibers significantly increased from 336.5±76.1 nm (40:70 ZA) to 820.3±330.3 nm (60:70 ZA) (Figure 3). These results are broadly in accordance with the literature in that the higher viscosity and lower conductivity both tend to predicate thicker nanofibers, with these characteristics also tending to reduce beading[6,11,30]. Decreasing the voltage to 20 kV caused a decrease in diameter (as can be seen by comparing the 40:70 ZA systems which were spun under both conditions); while the voltage is the driving stimulus for the deformation of the Taylor cone to form the fibers, hence high voltages ar often associated with lower diameters, increasing the voltage beyond a critical value can tend to result in poor and beaded fibers, hence an optimum exists for each system. Addition of plasticizers

did not have a profound effect on the morphology or diameter compared to the non-plasticized material.

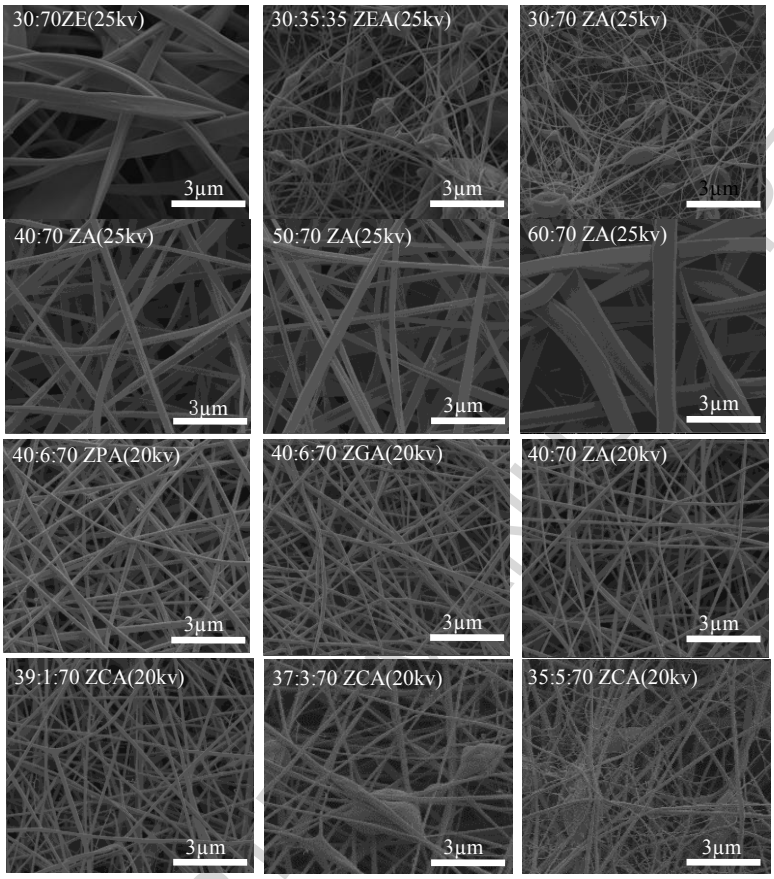

Figure 2. *SEM images of nanofibers prepared with different solvents, zein concentrations and additives (plasticizers and casein), at a constant voltage of 25 kV for different solvents and zein concentrations and 20 kV for different additives (plasticizers and casein).*

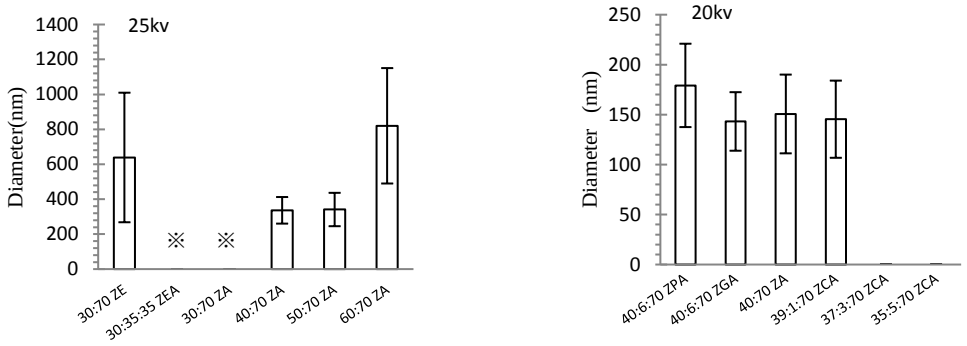

Figure 3. *Fiber diameters for nanofibers prepared with different solvents, zein concentrations and additives (plasticizers and casein), at a constant voltage of 25 kV for different solvents and zein concentrations and 20 kV for different additives (plasticizers and casein). ※indicates beaded fibers.*

When the amount of casein was increased above its minimum level, the conductivity decreased from 1.33±0.02 to 1.23±0.02mS, while the apparent viscosity at 300 s^{-1} of the solution dramatically increased from 0.29±0.02 to 0.77±0.05Pa.s. As mentioned above, a higher viscosity generally tends to facilitate the formation of fibers without beads. However, in this case, the presence of casein dominated the behaviour of the system, and the fibers changed from bead-free fibers (145.40±38.6 nm for 39:1:70 ZCA) to beaded fibers for 37:3:70 ZCA and 35:5:70 ZCA. It is interesting to note that, despite the favourable effect on viscosity, the addition of casein does not facilitate the formation of zein fibers in acetic acid. The poor electrospinning properties of casein have been previously documented[31]; it was reported that although casein in 5 wt% aqueous triethanolamine could form viscous solutions in the 10 to 30 wt% concentration range, none of these solutions could be successfully electrospun using the experimental conditions used. This was ascribed to their complex macromolecular and three-dimensional structures as well as strong inter- and/or intra- molecular forces[31] resulting in strong self-association, although the exact mechanism remains unclear. The increase in viscosity caused by addition of casein to the zein did not result in an improvement in fiber architecture, possibly reflecting the poor spinning properties of casein and the surface activity of this molecule which may have compromised the Taylor cone formed from the binary solutions.

Secondary structure of electrospun zein systems

In order to examine the effects of both processing and additive inclusion on the chemical structure of electrospun zein fibers, ATR-FTIR studies were conducted, particularly with a view to establishing whether any change in the ratio of α- to β-structure (turns and sheets) was apparent as a result of the process or formulation composition. The ATR-FTIR spectra of zein fibers electrospun using different solvents, zein concentrations and additives are shown in Figure 4. The characteristic peak at 1700–1600 cm^{-1} was assigned to the amide I band (C=O stretching with some contribution from the N-H vibration) and that at 1600–1500 cm^{-1} was assigned to the amide II band (NH bending combined with CN stretching)[32]. All ATR-FTIR spectra of electrospun zein fibers prepared with different solvents and zein concentrations showed the characteristic maximum of the amide I band at 1649cm^{-1}, with the amide II maximum appearing at 1535 cm^{-1}. Differences were seen, however, for electrospun zein fibers containing additives. The characteristic maxima of the amide I / amide II bands are shifted to the higher frequencies of 1652 cm^{-1}/1541cm^{-1} and 1650cm^{-1}/1541cm^{-1} for 40:6:70 ZPA and 40:6:70 ZGA, and to lower frequencies of 1647 cm^{-1}/1533cm^{-1} and 1645 cm^{-1}/1531cm^{-1} for 37:3:70 ZCA and 35:5:70 ZCA, respectively. The changes in frequency may reflect a change in a small amount of random coil structures present. Typically, random coils have maxima in the region between 1640 and 1649 cm^{-1} and may overlap the α-helical region. The increase in maximum observed may be due to a decrease in random structure and an increase in helical structure facilitated by the plasticizer, whilst the decrease may be due to the interaction with casein.

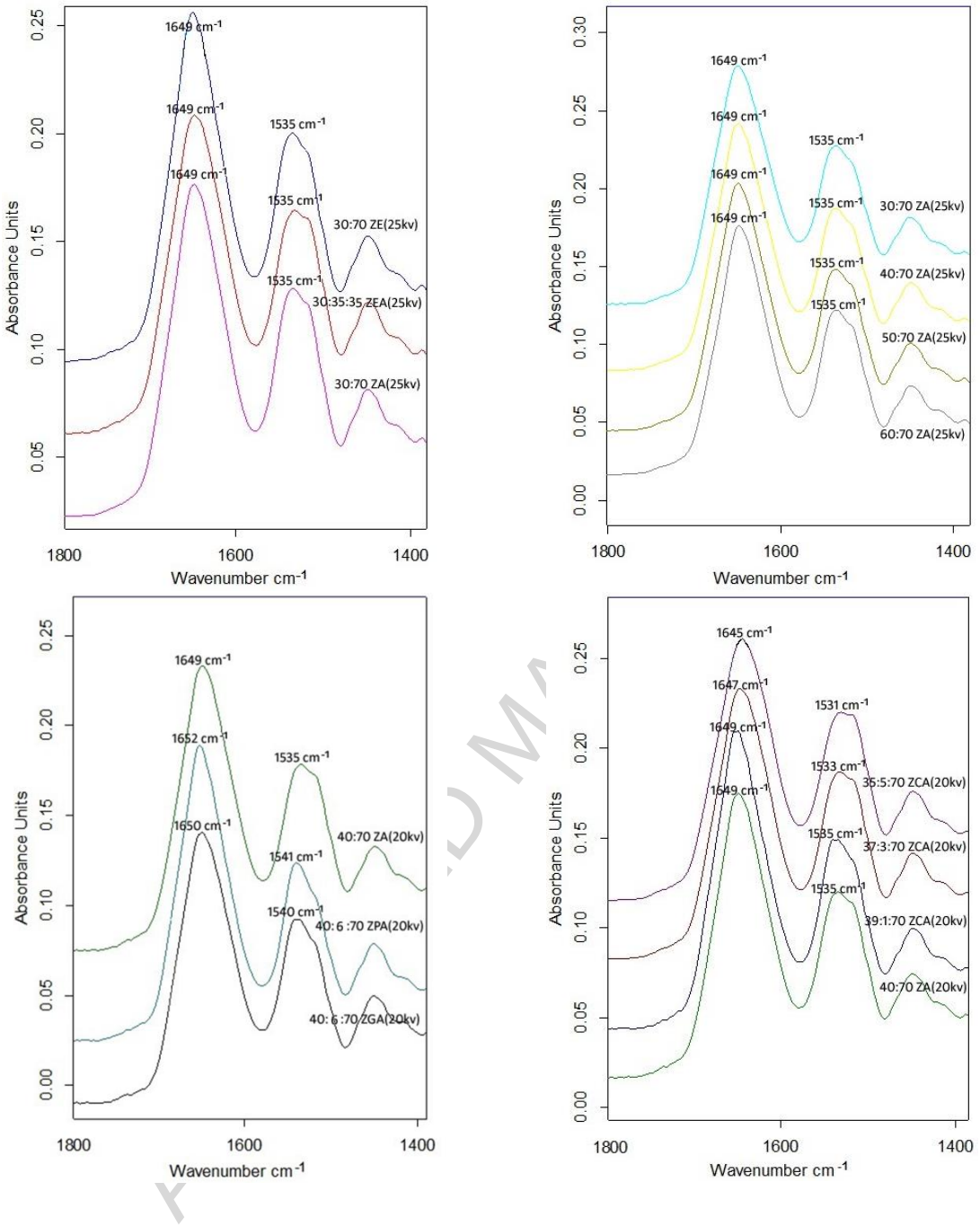

Figure 4. *ATR-FTIR spectra between 1700 and 1400 cm^{-1} for the electrospun zein nanofibers prepared with different solvents, zein concentrations and additives (plasticizers and casein), at a constant voltage of 25 kV for different solvents and zein concentrations and 20 kV for different additives (plasticizers and casein).*

These results show evidence for a direct interaction of the plasticiser or casein with zein. Moreover, the amide I band indicates a complex secondary structure which is composed of several

overlapping sub-structures such as side-chain, β-sheet, α-helix/random coil and β-turn of the protein, hence the secondary structures were estimated by second-derivative and Gaussian curve fitting of the amide I band in the regions of 1600−1700 cm^{-1} using Origin Pro 9.0 software. Representative deconvoluted peaks ranging between 1700 and 1600 $cm^{-1}$for zein fibers are shown in Figure 5.

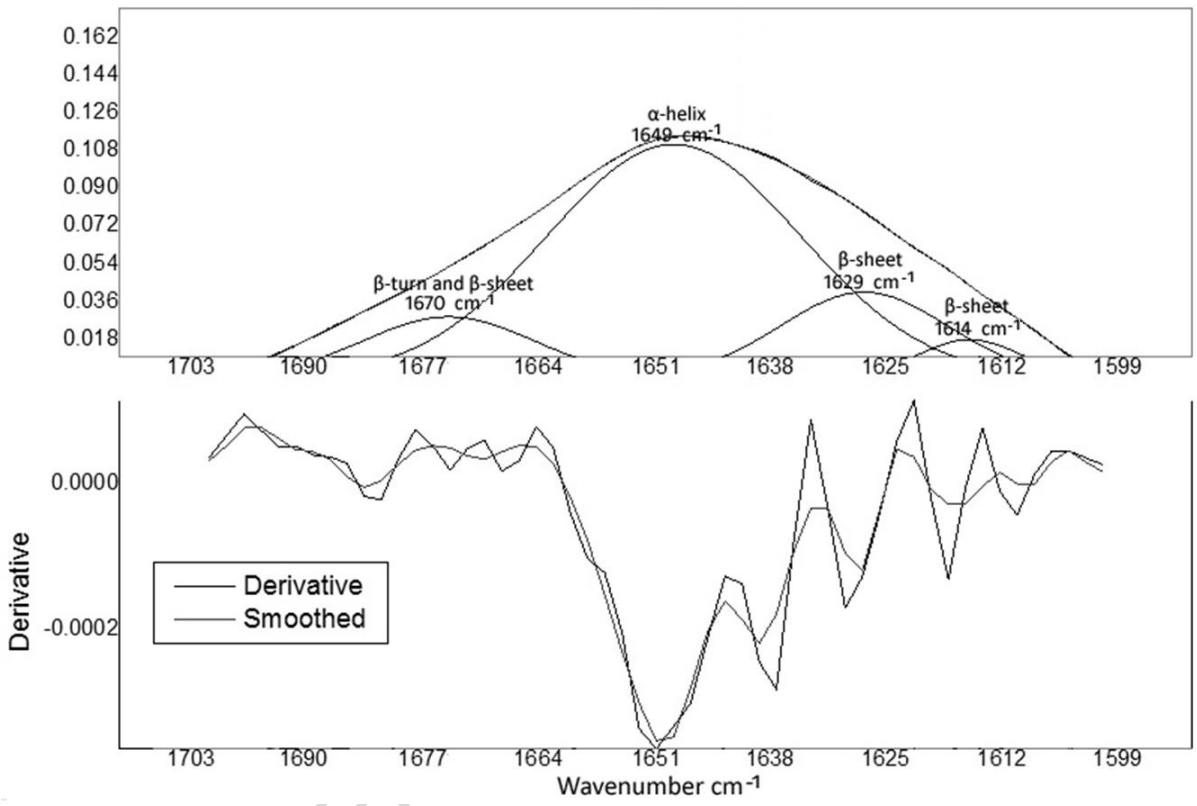

Figure 5. *The representative deconvoluted peaks of ATR-FTIR spectra ranging between 1700 and 1600 cm^{-1} for the electrospun zein nanofibers prepared with different solvents, zein concentrations and additives (plasticizers and casein), at a constant voltage of 25 kV for different solvents and zein concentrations and 20 kV for different additives (plasticizers and casein).*

It is interesting to characterise the changes in α-helical content of the fibers produced under the different conditions. This has been parameterised with the minimum number of Gaussian functions required to fit the peak shape. Four major bands in the amide I region were obtained based on the derivative spectra. The assignment of the bands shown in Figure 5 closely follows that reported earlier, with maxima being shown in brackets: β-turns and β-sheets (1670 cm^{-1}), α-

helix (possibly with a small random coil contribution) (1649 cm^{-1}), intramolecular β-sheets (1614 cm^{-1}) and intermolecular β-sheets (1629 cm^{-1})[32]. The α- helix to total β-structure ratios are shown in Figure 6.

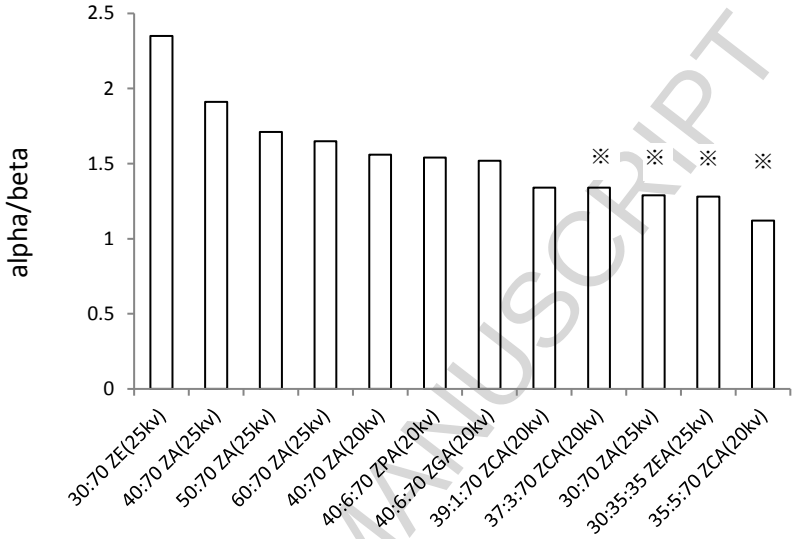

Figure 6. *The α-helix to total β-structure ratios in the electrospun zein nanofibers prepared with different solvents, zein concentrations and additives (plasticizers and casein), at a constant voltage of 25 kV for different solvents and zein concentrations and 20 kV for different additives (plasticizers and casein).※ indicates beaded fibers.*

Figure 6 shows differences in the ratios of α-helix to β-structure in electrospun zein nanofibers. The higher ratios of α- helices shown by 30:70 ZE (25 kV), 40:70 ZA (25 kV), 50:70 ZA (25 kV), 60:70 ZA (25 kV), 40:70 ZA (20 kV), 40:6:70 ZPA (20 kV) and 40:6:70 ZGA (20 kV) correspond to those fibers that did not show evidence of beading. In contrast, lower α- to β- ratios were associated with bead formation, despite the expectation that the higher β content may be associated with greater intermolecular interaction and hence greater viscosity which is normally associated with lower beading. It is also noted that the higher α content systems were also associated with the lower fiber diameters; this is consistent with the expectation that a lower viscosity is associated with lower dimeters.

Only small differences in protein secondary structure were seen among zein nanofibers containing the two plasticizers and the α- to β- ratio of these is less than in the 40:70 ZA (20 kv). Evidently, therefore, adding plasticiser at best weakly enhances the α-helix content of the protein. This is in contrast to the work of Gilgren et al[33] where addition of glycerol to zein significantly increased the α-helix content. However, the samples used by Gilgren et al[33] were produced as films from ethanol /water and the differences between their results and those presented here may reflect the different origins of the material under test.

Overall, therefore, the proportion of α- to β-structure may indeed be influenced by the electrospinning process and formulation, but perhaps surprisingly the most marked effects were seen for the different solvent systems. Comparison of 30:70 ZA(25 kV) with 30:70 ZE (25 kV) shows that changing the solvent from acetic acid to ethanol results in a 70% increase in the α- to β- ratio. However, increasing the concentration of the protein in acetic acid samples from 30% to 40% results in a 50% increase in this ratio. The addition of plasticisers results in a 38% protein solution in a mainly acetic acid solvent. The α-helix contents of these samples are close to that of 40:70 ZA (20kV), suggesting that any effect of the plasticizer is fairly weak and the response is due mainly to the zein concentration.

Very little has been published in terms of the relationship between formulation and secondary structure of electrospun zein fibers. Studies to date include Kanjanapongkul et al[34] who explored the relationship between the formation of the gel-like substance causing clogging in zein solution, finding no relationship with the secondary structure of zein. Our results indicate that a higher α-content may lead to a greater tendency for bead-free fiber formation.

TTM Measurements – thermal analysis of nanofibers

Despite the widespread use of electrospinning, comparatively little information is available regarding the thermal analysis of such systems due to the traditionally small sample sizes that tend to be produced, although with more modern production methods this difficulty has been largely overcome. Nevertheless, thermal analysis of nanosized samples does require some particular consideration and here we describe the use of transition temperature microscopy (TTM), a recently introduced localized thermal analysis technique that gives information on sample properties at the

sub-micron scale. Conventional bulk thermal analysis methods such as differential scanning calorimetry, thermomechanical analysis and dynamic mechanical analysis are widely used for materials analysis. However, these techniques can only measure average or aggregate properties of the entire sample, that sample usually being in the mg weight range. Nanothermal analysis (nanoTA) has been utilized in which a miniaturized thermal probe heats a localized region on the sample surface to measure its thermal properties such as crystalline melting points and glass transitions (or more accurately softening points). TTM is an extension of the nanoTA technique whereby the sample surface is imaged with an optical microscope and a series of nanoTA measurements are performed over a pre-selected two dimensional area. Each measurement is stopped when the probe penetrates into the surface due to softening of the material. The detected transition temperature is recorded and assigned a colour based on the selected palette; hence, an image is assembled based on transition temperatures.[35,36]

In the present case, we have applied the technique to interrogate the non-woven mats of fibres produced via the electrospinning process. The probe size, which typically would examine a region of some 400x400nm, has been applied to a sample of the fiber mat in a two dimensional raster pattern in order to explore the ability of the technique to examine changes in thermal transition temperatures on altering the composition, as well as to develop the potential of the technique as a means of examining nanofiber mats as a potential quality control tool. The technique essentially derives a two dimensional map of probe penetration temperatures, these being portrayed as a colour plot with the corresponding temperature scale indicated on the right hand side of the image.

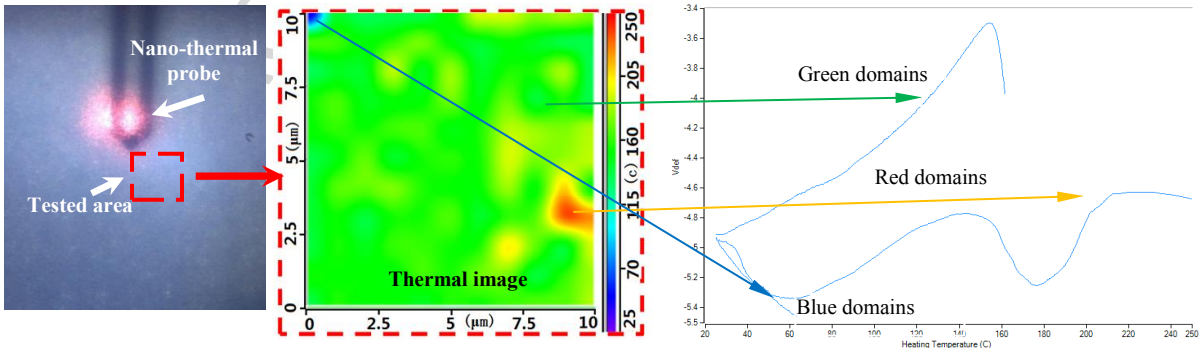

Figure 7. *TTM measurement on a 30:70 ZA (25 kv) sample. The optical image of the probe is shown on the left-hand side (the probe tip is therefore facing in to the image). The middle image shows the transition temperature map with the colour corresponding to the temperature scale on the right hand side (the image represents 10 μm x 10 μm) and the resulting nanoTA profiles of the tested regions are shown on the right-hand side.*

Figure 7 displays a representative image of a TTM measurement and data set. The probe has been landed on a mat comprising sample 30:70 ZGA (25 kv), hence the system is 'seeing' an effectively continuous structure. Figure 7 shows the probe taking the measurement, the localised thermal analysis response of probe position versus temperature corresponding to the different regions identified and the overall transition temperature map. The response is largely green dominated, which corresponds to a transition temperature of circa 154ºC (see the right hand x axis for the relationship between colour and temperature), close to the glass transition temperature of zein[37]. Two further domains may be seen in the image. The red domains refer to the higher of a double transition, the first corresponding again to the glass transition of the zein and the higher one seen at around 220ºC (i.e. the highest temperature is pixelated on the map). The latter corresponds to contact with the aluminium foil, hence this indicates the fiber is thin in the mesh and the probes penetrates through the mesh to the underlying foil. The blue regions represent a 'hole' in the mesh, whereby the probe appears to penetrate the sample at a low temperature. This is a phenomenon that has been previously observed in our laboratory whereby material is essentially pushed aside by the probe, leading to what appears to be incongruous penetration temperatures, and is an issue associated with materials whereby the positional integrity of the material under examination may be compromised by the measurement itself, although the penetration phenomenon tends to be well away from the transitions of interest and hence is not necessarily a significant problem. The technique is therefore able to provide a two dimensional compositional profile of the electrospun mat, based on the differences in transition temperatures of the different regions.

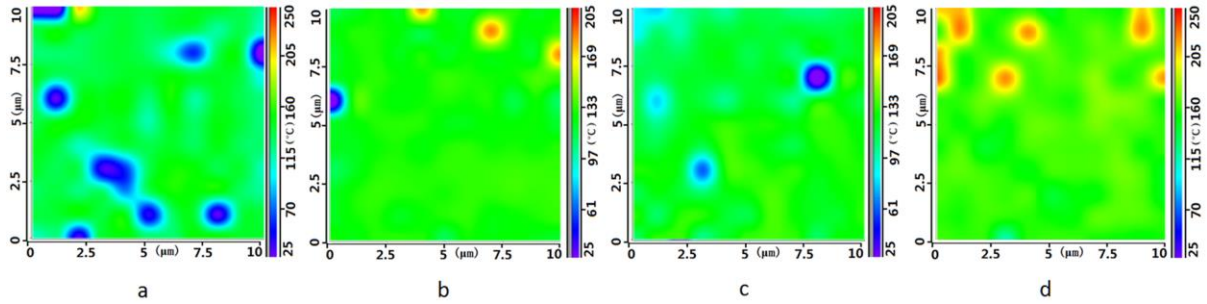

Figure 8. *TTM images of the electrospun zein nanofibers prepared with different solvents, zein concentrations and additives (plasticizers and casein), at a constant voltage of 25 kV for different solvents and zein concentrations and 20 kV for different additives (plasticizers and casein) (a) 30:70 ZE (25 kv); (b) 40:6:70 ZGA (20 kv); (c) 40:6:70 ZPA (20 kv); (d) 39:1:70 ZCA(20kv). Note the colour scale (right hand y axis) indicating the temperature corresponding to the colours used in the image.*

Figure 8 shows further images of mats studied using the technique. Examination of the right hand colour scale indicates that the two systems containing plasticizers (Figure 8b and 8c) show a significant decrease in the probe penetration temperature to circa 130^{o}C, reflecting the decrease in the glass transition temperature for these systems, while the casein system (Figure 8d) does not appear to demonstrate any significant lowering of the penetration temperature compared to the zein alone (Figure 8a). Given the use of fibers as macroscopic meshes (nonwoven or otherwise) in biomedical and increasingly drug delivery applications, such thermomechanical studies are of interest for both understanding plasticization effects and for predicting likely physical behavior in a biological environment. Work is ongoing to study the thermomechanical properties of individual fibers rather than the mats, although this initial study demonstrates the potential of the approach to allow insights into the glass transitional properties of the aggregated nanofiber systems.

CONCLUSIONS

The study has examined the compositional factors that may influence the integrity of zein nanofibers produced by electrospinning, with particular emphasis on the effects of solvent choice, zein concentration, plasticizer and casein inclusion. The interplay between composition, solution properties (viscosity and conductivity), fiber integrity and fiber thickness has been explored. ATR-FTIR was used to measure the effects of the process and inclusion of additives on the secondary

structure of the zein. In addition, the new technique of transition temperature microscopy has been introduced, which allows measurement of the penetration temperatures of the mats as a two dimensional map.

Zeins are undergoing something of a renaissance in their use within the biomedical field as an increasing number of drug delivery group in particular are seeking to exploit their safety and inert nature which, for many applications, renders them highly interesting as carriers and controlled release matrices for drugs whereby a sustained delivery regiment is required. In parallel to this, electrospinning is also gaining popularity within the field, particularly as high yield methods are being developed which render it possible for nanofibers to be produced at scale. This leaves a need for fundamental understanding of how zein fibers may be successfully produced and what characteristics may be important as their use extends into different delivery modalities. Here we highlight the potential importance of secondary structure and also the role of additives such as casein and plasticizers in their production and integrity, as well as the use of novel thermal methods for their characterization. In developing these systems as delivery vehicles, such physical characteristics will be important due to the implications for subsequent processing (e.g. tablet production, if desired) as well as activity within the body (for example if used as an implant whereby physical flexibility of the fibers may be a crucial characteristic). Overall, therefore, the study has highlighted the considerations for successful zein nanofiber production and also emphasized the need to consider the production, composition and integrity and physical properties in parallel as these systems move towards being used as viable biomedical and drug delivery vehicles.

ACKNOWLEDGEMENT

We wish to acknowledge the helpful input of Dr Bahijja Raimi-Abraham in the preparation of this manuscript.

AUTHOR INFORMATION

Corresponding Author: Duncan Craig

*E-mail: duncan.craig@ucl.ac.uk. Tel.: 44 207 7535819

Funding Sources

This work was supported by Reserve Talents of Universities Overseas Research Program of Heilongjiang and the Science Research Foundation of Heilongjiang University of Chinese Medicine (S201103).

REFERENCES

(1) Lawron JW 2002. Zein: A History of Processing and Use. Cereal Chem 79:1-18.

(2) Sukla R, Cheryan M 2001. Zein: the industrial protein from corn. Ind Crop Prod 2001 13:171-192.

(3) Yang JM, Zha LS, Yu DG, Liu, J 2013. Coaxial electrospinning with acetic acid for preparing ferulic acid/zein composite fibers with improved drug release profiles. Colloids Sur. B: Biointerfaces 102:737-743.

(4) Bugs MR, Forato LA, Bortoleto-Bugs RK, Fischer H, Mascarenhas YP, Ward RJ, Colnago, LA 2004. Spectroscopic characterization and structural modeling of prolamin from maize and pearl millet. Eur Biophys J 33:335-43.

(5) Forato LA, Bicudo T deC, Colnago LA 2003. Conformation of α zeins in solid state by FTIR spectroscopy. Biopolymers 72:421-426.

(6) Bhardwaj N, Kundu SC 2010. Electrospinning: a fascinating fiber fabrication technique. Biotechnol. Adv. 28:325-347.

(7) Sill TJ, Recum HA 2008. Electrospinning: applications in drug delivery and tissue engineering. Biomaterials 29:1989-2006.

(8) Jiang HL, Zhao PC, Zhu KJ 2007. Fabrication and characterization of zein-based nanofibrous scaffolds by an electrospinning method. Macromol Biosci 7:517-525.

(9) Brahatheeswaran D, Mathew A, Girija R, Nagaoka Y, Venugopal K, Yoshida Y, Maekawa T, Sakthikumar D 2012. Hybrid fluorescent curcumin loaded zein electrospun nanofibrous scaffold for biomedical applications. Biomed Mater 7:1-16.

(10) Neo YP, Ray S, Easteal AJ, Nikolaidis MG, Quek SY 2012. Influence of solution and processing parameters towards the fabrication of electrospun zein fibers with sub-micron diameter J Food Eng 109:645-651.

(11) Yao C, Li XS, Song TYJ 2007. Electrospinning and crosslinking of zein nanofiber mats. Appl Polym Sci 103:380-385.

(12) Jiang QR, Reddy N, Yang YQ 2010. Cytocompatible cross-linking of electrospun zein fibers for the development of water-stable tissue engineering scaffolds. Acta Biomateria 6:4042-4051.

(13) Kayaci F, Uyar T 2012. Electrospun zein nanofibers incorporating cyclodextrins. Carbohyd Polym 90:558-568.

(14) Lin JT, Li CH, Zhao Y, Hu J, Zhang LM 2012. Co-electrospun nanofibrous membranes of collagen and zein for wound healing. ACS Appl Mater Interfaces 4:1050-1057.

(15) Chen Y, Li XS, Song TY 2009. Preparation and characterization of zein and zein/poly-L-lactide nanofiber yarns. J Appl Polym Sci 114:2079-2086.

(16) Sergio TG, Ocio MJ, Lagaron JM 2009. Novel antimicrobial ultrathin structures of zein/chitosan blends obtained by electrospinning. Carbohydr Polym 77:261-266.

(17) Nie W, Yu DG, Branford-White C, Shen XX, Zhu LM 2012. Electrospun zein–PVP fibre composite and its potential medical application. Mater Res Innov 16:14-18.

(18) Alhusein N, Blagborough IS, Beeton ML, Bolhuis A, De Bank PA 2016. Electrospun zein/PCL fibrous matrices release tetracycline in a controlled manner, killing staphylococcus aureus both in biofilms and ex vivo on pig skin, and are compatible with human skin cells. Pharm Res 33:237-246.

(19) Brahatheeswaran D, Mathew A, Aswathy RG, Nagaoka Y, Venugopal K, Yoshida Y, Maekawa T, Sakthikumar D 2012. Hybrid fluorescent curcumin loaded zein electrospun nanofibrous scaffold for biomedical applications. Biomed Mat 7 1-16.

(20) Mejia CD, Mauer LJ, Hamaker BR 2007. Similarities and differences in secondary structure of viscoelastic polymers of maize α-zein and wheat gluten proteins. J. Cereal Sci. 45:353-359.

(21) Xu H, Chai Y, Zhang G 2012. Synergistic effect of oleic acid and glycerol on zein film plasticization. J Agric Food Chem 10 60:10075-10081.

(22) Gao C, Stading M, Wellner N, Parker ML, Noel TR, Mills EN, Belton PS 2006.Plasticization of a protein-based film by glycerol: a spectroscopic, mechanical, and thermal study. J Agric Food Chem 54:4611-4616.

(23) Lawton JW 2004. Plasticizers for zein: their effect on tensile properties and water absorption of zein films. Cereal Chem 81:1-5.

(24) Guo HX, Heinämäki J, Yliruusi J 2008. Stable aqueous film coating dispersion of zein. J Coll Interface Sci 322:478-84.

(25) Mejia CD, Gonzalez DC, Mauer LJ, Campanella OH, Hamaker BR 2012. Increasing and stabilizing β-sheet structure of maize zein causes improvement in its rheological properties. Agric Food Chem 60:2316-2321.

(26) Craig DQM, Kett VL, Royall PG, Andrews CS 2002. Pharmaceutical applications of micro-thermal analysis. J Pharm Sci 91:1201-1213.

(27) Deitzel JM, Kleinmeyer J, Harris D, Tan NCB 2001. The effect of processing variables on the morphology of electrospun nanofibers and textiles. Polymer 42:261-272.

(28) Mckee MG, Wilkes GL, Colby RH, Long TE 2004. Correlations of solution rheology with electrospun fiber formation of linear and branched polyesters. Macromolecules 37:1760-1767.

(29) Haghi AK, Akbari M 2007. Trends in electrospinning of natural nanofibers. Phys Status Solidi 204:1830-1834.

(30) Selling GW, Biswas, A, Patel A, Wallis DJ, Dunlao C, Wei Y 2007. Impact of solvent on electrospinning of zein and analysis of resulting fibers. Macromol Chem Phys 208: 1002-1010

(31) Xie JB, Hsiehy YL 2003. Ultra-high surface fibrous membranes from electrospinning of natural proteins: casein and lipase enzyme. J Mater Sci 38:2125-2133.

(32) Georget DMR, Belton PS 2006. Effects of temperature and water content on the secondary structure of wheat gluten studied by FTIR spectroscopy. Biomacromolecules 7:469-475.

(33) Gillgren T, Barker SA, Belton PS, Georget DMR, Stading, M 2009. Plasticization of zein: a thermomechanical, FTIR, and dielectric study. Biomacromolecules 10:1135–1139.

(34) Kanjanapongkul K, Wongsasulak S, Yoovidhya T 2010. Investigation and prevention of clogging during electrospinning of zein solution. J Appl Polym Sci 118:1821-1829.

(35) Meng J, Levina M, Rajabi-Siahboomi AR, Round AN, Reading M, Craig DQM 2012. The development of thermal nanoprobe methods as a means of characterizing and mapping plasticizer incorporation into ethylcellulose films. Pharm Res 29:2128-2138.

(36) Nikiforov MP, Gam S, Jesse S, Composto RJ, Kalinin SV 2010. Morphology mapping of phase-separated polymer films using nanothermal analysis. Macromolecules 43:6724-6730.

(37) Di Gioia L, Cuq B, Guilbert S 1999. Thermal properties of corn gluten meal and its proteic components. Int J Biol Macromol 24: 341-350

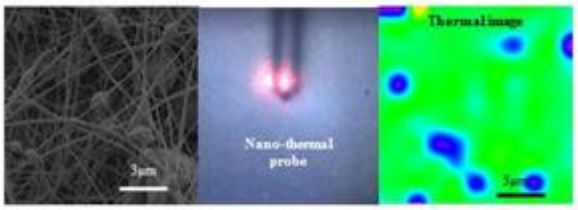

Scanning electron microscopy and transition temperature microscopy images of zein electrospun nanofibres

Graphical abstract